Strong Negative Thermal Expansion along the O−Cu−O Linkage in $CuScO_2$

J. Li,[†] A. Yokochi,[†] T. G. Amos,[‡] and A. W. Sleight*,[†]

Department of Chemistry, Oregon State University, Corvallis, Oregon 97331-4003, and NIST Center for Neutron Research, National Institute of Standards and Technology, 100 Bureau Drive, Stop 8562, Gaithersburg, Maryland 20899-8562

Received December 7, 2001. Revised Manuscript Received March 13, 2002

The structure of 2H $CuScO_2$ has been refined from single-crystal X-ray diffraction data obtained at room temperature and from neutron powder diffraction data obtained from 11 to 1206 K. Strong negative thermal expansion (-4.0×10^{-6}/K) has been found for the apparent Cu−O bond length below 300 K. This is the first example of strong negative thermal expansion in a metal oxide based on an O−M−O linkage instead of a M−O−M linkage. It is now the transverse thermal motion of Cu, instead of the transverse thermal motion of oxygen, that causes the negative thermal expansion. As expected for this mechanism for negative thermal expansion, the thermal displacement parameter for Cu is very pronounced perpendicular to the linear O−Cu−O linkage.

Introduction

The delafossite structure (Figure 1) exists for large families of $CuMO_2$ and $AgMO_2$ compounds where M is a trivalent cation in octahedral coordination.[1] Depending on the stacking along the *c* direction, 2H or 3R forms are observed. For the $CuMO_2$ series, M can range in size from Al to La. Several years ago, $CuMO_2$ phases were investigated as a possible route to superconductors.[2,3] In some $CuMO_2$ compounds the valency of Cu can be adjusted from 1.0 to 2.33 by oxygen intercalation. The copper atoms are in sheets as in all the cuprate superconductors. Nonetheless, superconductivity has never been found in any of these $CuMO_{2+x}$ phases. More recently, $CuMO_2$-type phases have been of interest as p-type transparent conductors.[4−7] Transparent thin films of $CuScO_{2+x}$ show a p-type conductivity of 30 S/cm at room temperature.[5] We have been investigating the structures of $CuScO_{2+x}$ phases. Here, we report on the structure of 2H $CuScO_2$ from 11 to 1206 K.

Experimental Section

Our synthesis method for 2H $CuScO_2$ free of the 3R form has previously been reported.[1] Neutron powder diffraction data were collected using the BT-1 32-counter high-resolution diffractometer at the NIST Center for Neutron Research at the National Institute of Standards and Technology. A Cu (311) monochromator, yielding a wavelength of 1.5402(2) Å, was employed. Collimation of 15′, 20′, and 7′ of arc were used before and after the monochromator and after the sample, respectively. Data were collected at room temperature over a 2θ range of 3−168°. The sample was sealed in a vanadium container of length 50 mm and diameter of 15.6 mm inside a dry He-filled glovebox. A vacuum furnace was used for measurements above room temperature, and a closed-cycle He refrigerator was used for temperatures below room temperature. The data were corrected for absorption[8] and refined by the Rietveld method using both Fullprof[9] and GSAS[10] software.

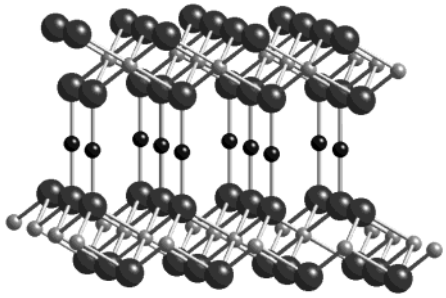

Figure 1. Delafossite structure. Small, dark atoms are Cu; small, light atoms are Sc; large atoms are O.

Single crystals of 2H $CuScO_2$ were grown in a PbO flux in a Cu crucible under Ar using a 2:1 PbO:$CuScO_2$ molar ratio. The sample was heated at 323 K/h to 1223 K. The cooling rate from this temperature was 275 K/h until 1093 K and then 303 K/h to room temperature. Single-crystal X-ray diffraction data were obtained at room temperature on a Rigaku AFC6R diffractometer with monochromatic Mo Kα radiation (λ = 0.71069 Å). No decay in intensity was noted during data collection. The observed intensities were corrected for Lorentz

* To whom correspondence should be addressed. E-mail: arthur.sleight@orst.edu.
[†] Oregon State University
[‡] NIST.

(1) Nagarajan, R.; Duan, N.; Jayaraj, M. K.; Li, J.; Vanaja, K. A.; Yokochi, A.; Draeseke, A.; Tate, J.; Sleight, A. W. *Int. J. Inorg. Mater.* **2001**, *3*, 265.
(2) Cava, R. J.; Zandbergen, H. W.; Ramirez, A. P.; Takagi, H.; Chen, C. T.; Krajewski, J. J.; Peck, W. F., Jr.; Waszczak, J. V.; Meigs, G.; Roth, R. S.; Schneemeyer, L. F. *J. Solid State Chem.* **1993**, *104*, 437.
(3) Cava, R. J.; Peck, W. F., Jr.; Krajewski, J. J.; Cheong, S.-W.; Hwang, H. Y. *J. Mater. Res.* **1994**, *9* (2), 314.
(4) Kawazoe, H.; Yasukawa M.; Hyodo H.; Kurita M.; Yanagi, H.; Hosono, H. *Nature* **1997**, *389*, 939.
(5) Duan, N.; Sleight, A. W.; Jayaraj, M. K.; Tate, J. *Appl. Phys. Lett.* **2000**, *77*, 1325.
(6) Nagarajan. R.; Draeseke, A. D.; Sleight, A. W.; Tate, J. *J. Appl. Phys.* **2001**, *89*, 8022.
(7) Jayaraj, M. K.; Draeseke, A. D.; Tate, J.; Sleight, A. W. *Thin Solid Films* **2001**, *397*, 244.
(8) *International Tables for X-ray Crystallography, Vol II Mathematical Tables*; Kasper, J. S., Lonsdale, K., Eds.; The Kynoch Press: Birmingham, 1959; pp 295−297.
(9) Rodriguez-Carvajal, J. FULLPROF: A program for Rietveld Refinement and Pattern Matching Analysis. In *Abstracts of the Satellite Meeting on Powder Diffraction of the XV Congress of the IUCr*, Toulouse, France, 1990; p 127.
(10) Larson, A. C.; Von Dreele, R. B. *LANSCE*; Los Alamos National Laboratory: Los Alamos, NM, 1994.

10.1021/cm011633v CCC: $22.00
Published on Web 04/19/2002

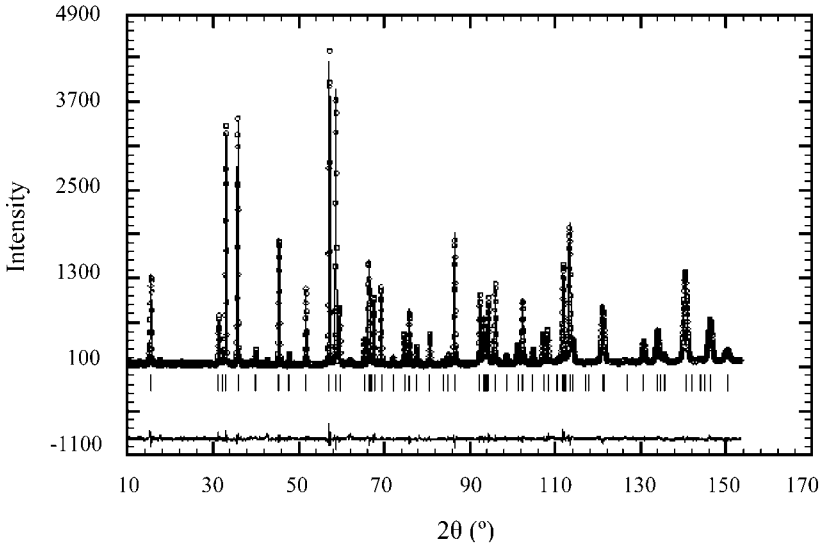

Figure 2. Observed (open circles), calculated (solid line), and difference profiles (below) for $CuScO_2$ at room temperature.

Table 1. Crystal Data and Structure Refinement for $CuScO_2$ Single Crystal

space group	$P6_3/mmc$
formula	$CuScO_2$
formula weight	140.50
temperature	290(2) K
wavelength	0.710693 Å
unit cell dimensions	$a = 3.215(1)$ Å $c = 11.386(1)$ Å
volume	101.89(5) Å^3
Z	2
density (calculated)	4.579 Mg/m^3
absorption coefficient	13.357 mm^{-1}
$F(000)$	132
crystal size	0.10 × 0.10 × 0.10 mm^3
θ range for data collection	3.58−49.99°
index ranges	$-6 \le h \le 6$, $-6 \le k \le 6$, $-1 \le l \le 24$
reflections collected	2112
independent reflections	246 [R(int) = 0.0237]
completeness to $\theta = 49.99°$	91.9%
absorption correction	empirical, Sortav as programmed in WinGX
max. and min. transmission	0.3622 and 0.7758
refinement method	full-matrix least-squares on F^2
data/restraints/parameters	246/0/9
goodness-of-fit on F^2	1.255
final R indices [$I > 2\sigma(I)$]	$R = 0.0187$, $wR = 0.0351$
R indices (all data)	$R = 0.0235$, $wR = 0.0358$
extinction coefficient	0.8(3)
largest diff. peak and hole	0.955 and −1.999 e/Å^3
z(O)	0.08928(7)

polarization and absorption. Data reduction was carried out using a local program, capable of creating a data file containing the crystal-dependent direction cosines of the diffracted and reverse incident beam, for purposes of correction of absorption anisotropy problems. Correction for the effects of absorption anisotropy was carried out using the program SORTAV,[11] as programmed in the software collection WinGX v1.64.02.[12] Structure solution was carried out using Patterson map interpretation as programmed in SHELXS-90 and refined using full-matrix least-squares refinement on F^2 using the program SHELXL-97.[13] Further data collection details are in Table 1.

Results

The structure for 2H $CuScO_2$ is described in space group $P6_3/mmc$ with Sc at 0 0 0, Cu at $^1/_3$ $^2/_3$ $^1/_4$, and oxygen at $^1/_3$ $^2/_3$ z where z is ≈0.09. Results of the single-crystal refinement are in Tables 1 and 2. Rietveld refinements of the neutron diffraction data at the various temperatures gave Rp in the range 4.4−5.4, Rwp 5.5−6.0, and χ^2 1.4−1.8. Le Bail fits to the same data gave fit parameters about 10% better. A typical plot of the observed and calculated intensities is given in Figure 2. Refined thermal displacement factors are plotted in Figure 3. All increase monotonically with increasing temperature. The U_{33} values for both Cu and O become negative at the lowest temperatures. For oxygen this can be ignored because the U_{11} values are within a couple of standard deviations of zero. The negative U_{33} values for Cu cannot be ignored because U_{33} for Cu has become 6 times the standard deviation at the lowest temperature. This apparent failure of the thermal ellipsoid model will be discussed later in this paper. Within the thermal ellipsoid model we can conclude that thermal motion along z becomes immeasurably small at low temperatures for both Cu and O.

Table 2. Anisotropic Displacement Parameters (Å^2 × 10^3) for $CuScO_2$[a]

	Cu	Sc	O		Cu	Sc	O
U_{11}	**14.8(3)**[b]	**4.5(1)**	**5.4(3)**	U_{33}	**0.4(4)**	**6.5(2)**	**2.5(4)**
	28(1)	18(1)	20(1)		18(1)	21(1)	19(1)

[a] The anisotropic displacement factor exponent takes the form: $-2\pi^2[h^2a^{*2}U_{11} + ... + 2hka^*b^*U_{12}]$. For all atoms $U_{22} = U_{11}$, $U_{12} = {}^1/_2U_{11}$, and $U_{23} = U_{13} = 0$. [b] Bold values are from neutron diffraction; others are from single-crystal X-ray diffraction.

In Figure 4 the unit cell edges and volume are plotted vs temperature. The behavior exhibited by the a cell edge can be considered typical thermal expansion behavior. For the c cell edge, negative thermal expansion occurs from 11 to 300 K. Above 300 K normal positive thermal expansion is observed. The combined effect of negative thermal expansion for c and positive thermal expansion for a yields a negative volume expansion only below 50 K.

(11) Blessing, R. H. *Acta Crystallogr., Sect A* **1995**, *51*, 33.
(12) Farrugia, L. J. *J. Appl. Crystallogr.* **1999**, *32*, 837.
(13) Sheldrick, G. M. *SHELX97 [Including the programs SHELXS97, SHELXL97, and CIFTAB]—Programs for Crystal Structure Analysis* (Release 97-2); Institüt für Anorganische Chemie der Universität: Göttingen, Germany, 1998.

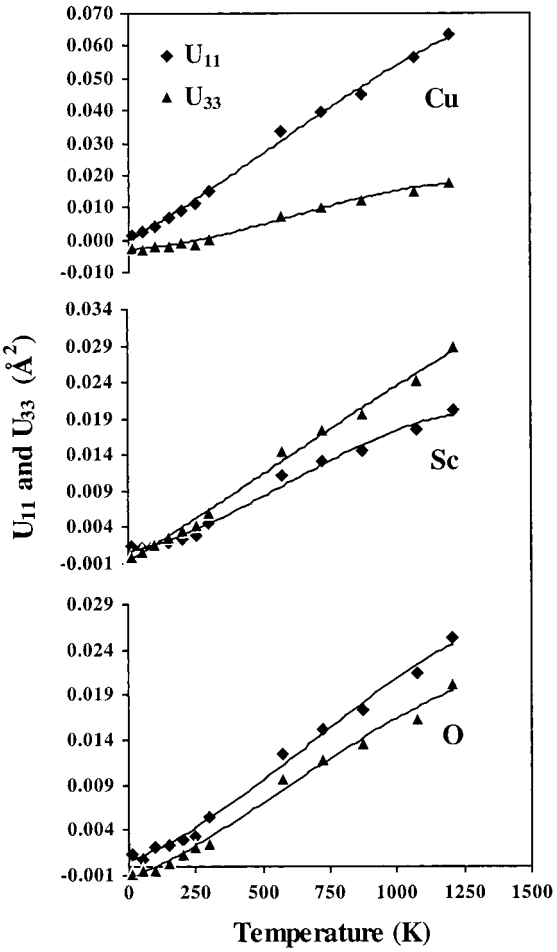

Figure 3. Variation of thermal displacement factors with temperature.

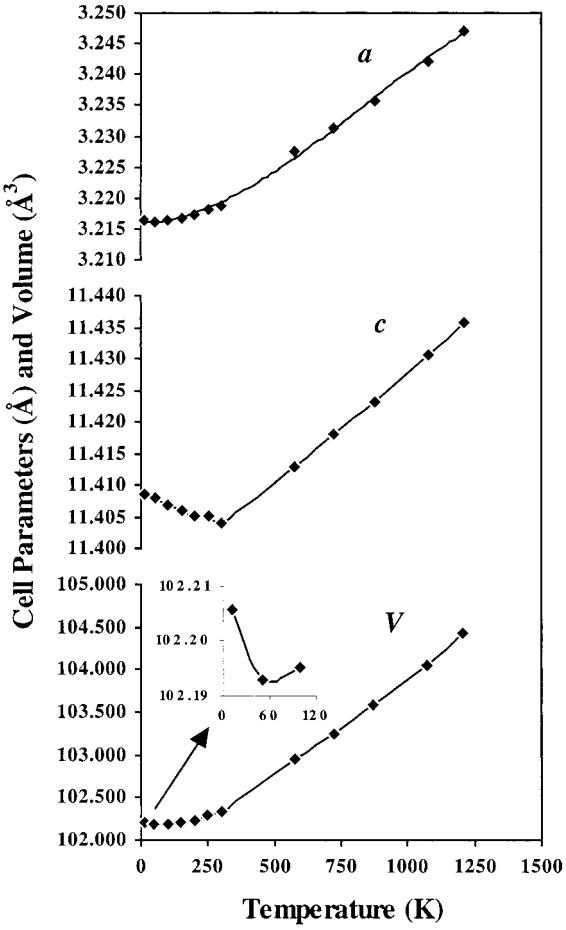

Figure 4. Variation of unit cell edges and volume with temperature.

The cause of the negative thermal expansion of the *c* cell edge is apparent in Figure 5. There is a strong negative thermal expansion of the apparent Cu−O bond length from 11 to 300 K. This is for an O−Cu−O linkage parallel to the *c* axis. Thermal expansion of the Sc−O bond vs temperature (Figure 5) can be considered normal, and this is directly related to the thermal expansion of the *a* cell edge. Figure 6 shows the Cu−Cu distance vs temperature. This is also the value of the Sc−Sc distance vs temperature. One of the O−O distances is the same as the Cu−Cu and Sc−Sc distances. This is an O−O pair that does not define a shared edge for the ScO_6 octahedra. The O−O distance across the shared edge is considerably shorter (Figure 6), as expected. Bond angles vs temperature are given in Figure 7. The O−Sc−O angles are equivalent to the Sc−O−Sc angle because of lattice symmetry.

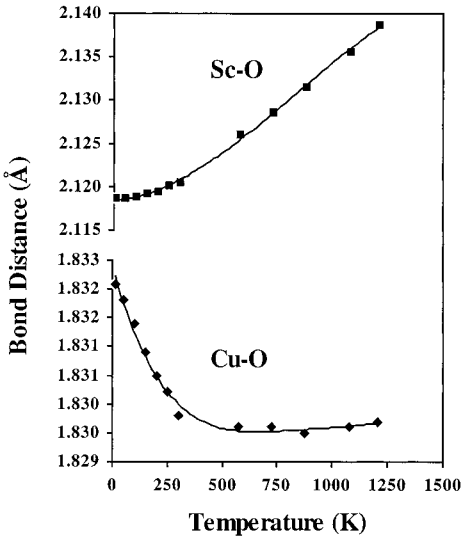

Figure 5. Variation of Cu−O and Sc−O bond lengths with temperature.

Discussion

In recent years negative thermal expansion has been found in many metal oxides.[14] The mechanism for this unusual behavior is usually related to the transverse thermal motion of oxygen in M−O−M linkages. Another possibility for negative thermal expansion in an oxide could be based on a cation in 2-fold coordination to oxygen, that is, O−M−O linkages. This cation coordination is rare except for d^{10} cations such as Cu(I), Ag(I), and Hg(II). The structure of Cu_2O contains linear O−Cu−O linkages, and the thermal expansion of Cu_2O below 323 K is negative but very low, -0.6×10^{-6}/K.[15] Above 323 K the thermal expansion coefficient of Cu_2O is very low but positive, $+0.25 \times 10^{-6}$/K. The structure of Ag_2O is the same as Cu_2O, thus again having the

(14) Sleight, A. W. *Inorg. Chem.* **1998**, *37*, 2854.

(15) Taylor, D. *Br. Ceram. Trans. J.* **1985**, *84* (1), 9.

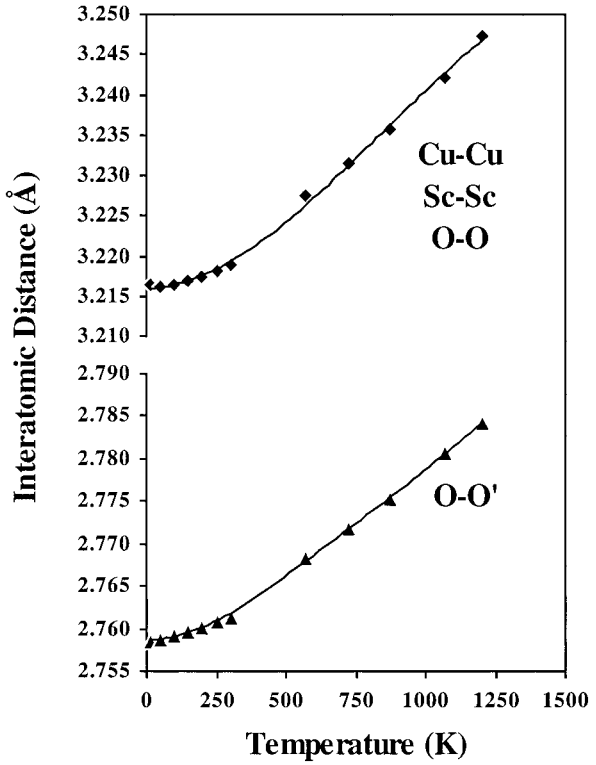

Figure 6. Variation of metal−metal and O−O interatomic distances with temperature.

cation in 2-fold linear coordination to oxygen. The thermal expansion coefficient for Ag_2O over the measured temperature range of 150−520 K is large, +39.4 $\times$ 10^{-6}/K.[15] Therefore, having a cation in 2-fold linear coordination does not necessarily lead to negative thermal expansion.

In cubic Cu_2O the thermal expansion coefficient for the Cu−O bond is the same as that for the unit cell edges. Thus, the negative expansion for Cu_2O, -0.6×10^{-6}/K, is much less pronounced than the negative thermal expansion for the Cu−O bond in $CuScO_2$ below room temperature, -4.0×10^{-6}/K. Assuming interference of the transverse thermal motion of Cu with its Cu neighbors, the reason for this might be the much larger Cu−Cu distance in $CuScO_2$, 3.22 Å, compared to 3.02 Å in Cu_2O. Apparently, there are no other measurements of the Cu(I)−O bond thermal expansion below room temperature. There is, however, a measurement of the thermal expansion of the Cu(I)−O bond above room temperature in $CuAlO_2$.[16] This expansion in $CuAlO_2$ is 5.4×10^{-6}/K whereas it is only 1.1×10^{-6}/K in $CuScO_2$. Brown et al.[17] have pointed out that the thermal expansion of the Cu−O bond in $CuAlO_2$ is much less than expected on the basis of bond valence considerations. Thus, the thermal expansion of the Cu−O bond in $CuScO_2$ above room temperature can be considered exceptionally low. Assuming that the low thermal expansion of the apparent Cu−O distance is related to the transverse thermal motion of Cu in the O−Cu−O linkage, we can again invoke interference with this motion by neighboring Cu atoms. The Cu−Cu distance

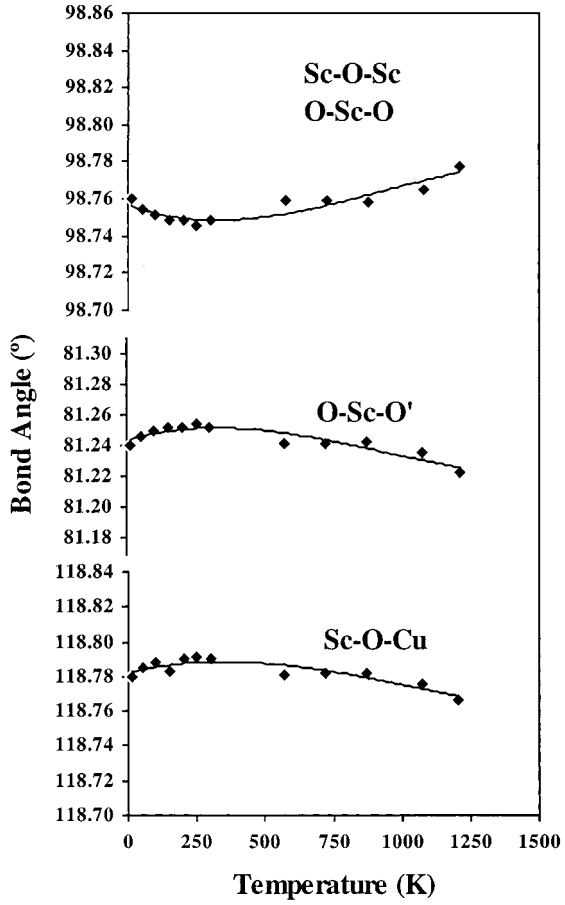

Figure 7. Variation of bond angles with temperature.

in $CuAlO_2$ is only 2.86 Å compared to the 3.22-Å value in $CuScO_2$. This is also consistent with the Cu U_{11} values from single-crystal X-ray diffraction at room temperature. Our value for $CuScO_2$ (Table 2) is 2 times greater than three published values for $CuAlO_2$.[17−19] Although the thermal expansion coefficient for the Cu−O bond below room temperature is -4.0×10^{-6}/K, the thermal expansion of the *c* cell edge over this temperature range is only -1.3×10^{-6}/K because of compensation by the positive thermal expansion of the Sc−O bond (Figure 5).

The negative U_{33} values for Cu below room temperature suggest that the thermal motion of Cu should be described as a torus instead of a thermal ellipsoid. This is a conclusion reached by other workers[20] in the case of oxygen in Sc−O−W linkages in $Sc_2W_3O_{12}$, a compound that we found exhibits negative thermal expansion.[21] We therefore explored a torus model for the thermal motion of Cu. This was done by placing 3, 6, or 12 Cu atoms around the 6-fold axis and refining the torus radius using an isotropic displacement parameter for Cu. All three torus models and the ellipsoid model gave essentially the same agreement factors at all temperatures. The results are given in Figure 8 along

(16) Ishiguro, T.; Ishizawa, N.; Mizutani, N.; Kato, M. *J. Solid State Chem.* **1982**, *41*, 132.
(17) Brown, I. D.; Dabkowski A.; McCleary, A. *Acta Crystallogr., Sect B* **1997**, *53*, 750.
(18) Ishiguro, T.; Ishizawa, N.; Mizutani, N.; Kato, M. *Acta Crystallogr., Sect. B* **1983**, *39*, 564.
(19) Ishiguro, T.; Kitazawa, A.; Mizutani, N.; Kato, M. *J. Solid State Chem.* **1981**, *40*, 170.
(20) Weller, M. T.; Henry, P. F.; Wilson, C. C. *J. Phys. Chem. B* **2000**, *104*, 12224.
(21) Evans, J. S.; Mary, T. A.; Sleight, A. W. *J. Solid State Chem.* **1998**, *137*, 148.

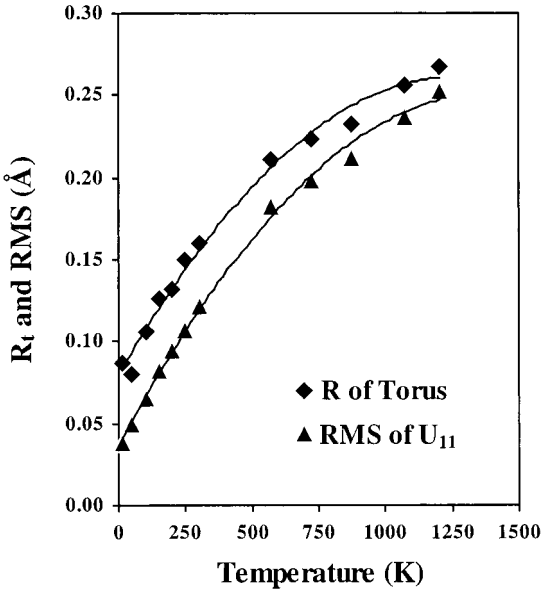

Figure 8. Root-mean-square displacement values and torus radii as a function of temperature.

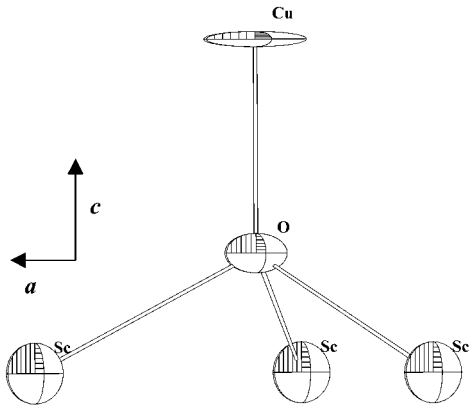

Figure 9. Partial view of $CuScO_2$ structure at room temperature showing thermal ellipsoids.

with root-mean-square (rms) displacements calculated from the thermal ellipsoid U_{11} values. As might be expected, the torus values are somewhat larger than the rms values. Although we cannot distinguish between the torus model and the thermal ellipsoid model on the basis of agreement factors, the torus model is a physically reasonable model at all temperatures whereas the U_{33} parameter for Cu in the ellipsoid model is physically impossible below room temperature. Even at room temperature, the shape of the thermal ellipsoid for Cu is extreme (Figure 9). The thermal motion of Cu perpendicular to the O−Cu−O linkage is not unusually high, but the Cu motion along the Cu−O bond is very low.

Structural refinements of $CuMO_2$ delafossites based on single-crystal X-ray diffraction data are available for M = Al, Ga, Fe, Rh, Sc, and Y.[17−19,22−25] Such studies are also available for $YBa_2Cu_3O_6$,[26−29] $PrBa_2Cu_3O_6$,[30] $PbCu_2O_2$,[31] Cu_4O_3,[32] and Cu_2O.[33−35] All of these compounds have linear O−Cu(I)−O linkages, and the Cu thermal motion perpendicular to these linkages is always considerably higher than that along the Cu−O bond. This is the expected behavior, but our attempts to find a correlation of U_{11} or U_{11}/U_{33} with Cu−Cu distance or Cu−O distance failed. This may in large part simply reflect the unreliability of the U values from routine X-ray diffraction studies. This problem is indicated in Table 2 where our room temperature U values obtained from powder neutron diffraction data are significantly different from those found from our single-crystal X-ray diffraction data.

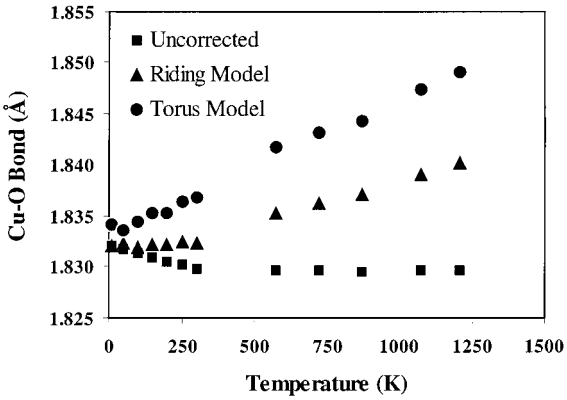

Figure 10. Cu−O bond distances vs temperature showing riding model and torus model corrections.

It has long been recognized that apparent bond lengths should be corrected for thermal motion, especially when the thermal motion is high. The most conservative correction would be the correction assuming a riding motion.[36] The results of this correction are shown in Figure 10. In this model the two oxygen atoms of the O−Cu−O linkage move in the same direction as Cu when Cu is moving transverse to the O−Cu−O linkage. This correction alone is enough to completely eliminate the negative thermal expansion behavior of the Cu−O bond. The correction based on the torus model is much larger (Figure 10), mainly because the oxygen atoms are considered to be stationary in this model. In this model the thermal expansion of the Cu−O bond is $+5.46 \times 10^{-6}$/K over a broad temperature range. This is a very common thermal expansion for a metal−oxygen bond distance.

Acknowledgment. This work was supported by NSF.

Supporting Information Available: Crystallographic data (CIF). This material is available free of charge via the Internet at http://pubs.acs.org.

CM011633V

(22) Kohler, B. U.; Jansen, M. *Z. Anorg. Allg. Chem*. **1986**, *543*, 73.
(23) Effenberger, H. *Acta Crystallogr., Sect C* **1991**, *47*, 2644.
(24) Subramanian, M. A.; Marshall, W. E. I. Du Pont De Nemours & Co., Inc.., unpublished data.
(25) Ishiguro, T.; Ishizawa, N.; Mizutani, N.; Kato, M. *J. Solid State Chem*. **1983**, *49*, 232.
(26) Jang, W.-J.; Mori, H.; Watahiki, M.; Tajima, S.; Koshizuka, N.; Tanaka, S. *J. Solid State Chem*. **1997**, *130*, 42.
(27) Garbauskas, M. F.; Green, R. W.; Arendt, R. H.; Kasper, J. S. *Inorg. Chem*. **1988**, *27*, 871.
(28) Roth, G.; Renker, B.; Heger, G.; Hervieu, M.; Domenges, B.; Raveau, B. *Z. Phys. B, Condens. Matter* **1987**, *69*, 53.
(29) Swinnea, J. S.; Steinfink, H. *J. Mater. Res*. **1987**, *2* (4), 424.
(30) Lowe-Ma, C. K.; Vanderah, T. A. *Physica C (Amsterdam), PHYCE* **1992**, *201*, 233.
(31) Szillat, H.; Teske, C. L. *Z. Anorg. Allg. Chem*. **1994**, *620*, 1307.
(32) Keeffe, M. O.; Bovin, J. O. *Am. Mineral*. **1978**, *63*, 180.
(33) Lippmann, T.; Schneider, J. R. *Acta Crystallogr., Sect A* **2000**, *56*, 575.
(34) Kirfel, A.; Eichhorn, K. *Acta Crystallogr., Sect A* **1990**, *46*, 271.
(35) Restori, R.; Schwarzenbach, D. *Acta Crystallogr., Sect B* **1986**, *42*, 201.
(36) Busing, R. W.; Levy, H. A. *Acta Crystallogr*. **1964**, *17*, 142.